

Localized deposition of zinc oxide films by automated fluid dispensing method

Karel Domansky ^{a,*}, Aimee Rose ^b, William H. Grover ^c, Gregory J. Exarhos ^a

^a Pacific Northwest National Laboratory, Richland, WA 99352, USA

^b Department of Chemistry, Massachusetts Institute of Technology, Cambridge, MA 02139-4307, USA

^c Department of Chemistry, University of Tennessee, Knoxville, TN 37996, USA

Received 30 December 1999; accepted 3 February 2000

Abstract

Optically clear Au- and Ga-doped zinc oxide films have been locally deposited from solution precursors on silicon and silica substrates as micrometer size dots using an automated fluid dispensing method. Dot dimensions have been shown to be strongly dependent on the solution composition and substrate temperature. Solution-dispensed films have been characterized by means of optical transmission and reflectance spectroscopy, spectroscopic ellipsometry, and profilometry measurements. Trivalent Au- and Ga-doped zinc oxide features about 500 μm in diameter were deposited on chemically-sensitive field-effect transistors (CHEM-FET). Contrasting behavior in measured work function and film resistance was found for Au and Ga doped films upon exposure to hydrogen and ammonia. © 2000 Published by Elsevier Science S.A. All rights reserved.

Keywords: Localized film deposition; Automated fluid dispensing; Zinc oxide; Chemical sensor; CHEMFET

1. Introduction

Zinc oxide films can be prepared by numerous methods including spray pyrolysis [1–3], chemical vapor deposition (CVD) [4], sputtering [5,6], evaporation [7], laser induced deposition [8], and spin casting from solution precursors [9]. An advantage common to all of these methods is that uniform films can be deposited on large substrates. For some applications, such as sensors, zinc oxide films must be either patterned [10] or locally deposited on smaller selected areas of a substrate. Patterning can be done by conventional methods, employing photoresist and etching. However, this adds several processing steps in addition to film deposition. An alternative approach to the deposition of metal oxide films involves localized thermal activation CVD [11]. This technique is possible only when specialized heating structures are built into the substrate. If more than one material is deposited onto a substrate, cross contamination of films from different precursor vapor species

must be prevented. Spatially resolved metal oxide film structures also have been locally formed by densification through laser irradiation of spin cast solution precursors and subsequent dissolution of the material outside of the irradiating laser footprint [12]. However, thermal diffusion can induce cross contamination as in the CVD process and localized heating can result in substrate damage.

Recent work in this laboratory [9,13] has shown that spin casting methods can be used to deposit optically clear ZnO films from either aqueous or alcoholic precursor solutions which are subjected to a 5-min anneal at 400°C. In this work, we describe a method to deposit micrometer size zinc oxide features using solution precursors and an automated fluid dispensing. As in the spin casting technique, heating subsequent to deposition produces an optically clear zinc oxide film. This method allows spatially resolved structures forming onto cleaned substrates without any additional processing steps and also prevents cross contamination.

Zinc oxide films deposited on silica and silicon substrates were characterized using several nondestructive optical methods. Transmission measurements and spectroscopic ellipsometry were used to determine the opti-

* Corresponding author. Present address: Department of Bioengineering and Environmental Health, Massachusetts Institute of Technology, Room 16-451a, Cambridge, MA 02139, USA.

cal constants and film thickness. To demonstrate the potential of this deposition approach, Au- and Ga-doped zinc oxide dots with diameters on the order of 500 nm were deposited onto chemically-sensitive field-effect transistors (CHEMFETs) [14]. Although the maximum long-term operating temperature of these devices is well below that normally used in zinc oxide sensors [15], marked changes in work function (WF) and film resistance were measured upon exposure to hydrogen and ammonia.

While this work demonstrates a fluid dispensing route to the deposition of zinc oxide film structures, the method is applicable for the deposition of other metal oxide film structures comprised of zirconium dioxide [12] or tin oxide. Additionally, zinc or other metal oxides with different types and levels of doping can be deposited in close proximity. This is essential for applications such as integrated chemical sensor arrays where it is desirable to deposit a variety of doped films on a single substrate to introduce chemical diversity into the array. Using this dispensing technique, materials can be deposited as thin films onto selected locations only. Therefore, cross-contamination caused by contact with masking materials or multiple solution precursors can be eliminated.

2. Experimental

2.1. Solution preparation

A 1 M solution of zinc acetylacetonate in a 30% ethanol–water mixture was prepared. One atomic % Au from $\text{HAuCl}_4 \cdot 3\text{H}_2\text{O}$ or 1 atomic % Ga from $\text{Ga}_2(\text{NO}_3)_3 \cdot 9\text{H}_2\text{O}$ was added for Au and Ga doping, respectively. A small addition of glacial acetic acid slightly acidified the basic alcohol solution to completely dissolve the zinc acetylacetonate [16] and prevent precursor precipitation. The solution was stirred and heated at 60°C, cooled to room temperature (r.t.), and filtered through a 0.45- μm pore size Teflon filter. Subsequent dilutions of these solutions were used in dispensing different dot sizes and thickness. A 1:10 dilution with ethanol was used to dispense dots for optical characterization. Several layers were deposited to create a film thick enough for transmission and reflectance measurements. A 1:10 dilution with water was used for dispensing zinc oxide on CHEMFET.

2.2. Instrumentation

Zinc oxide films were deposited using an automated fluid dispensing system (Model A402B, Asymtek, Carlsbad, CA) equipped with AV-500 targeting offset camera and DV-01 syringe valve bracket. The system allows materials to be deposited as dots, continuous lines, or

arcs with a 25- μm spatial resolution. The zinc oxide solution precursors were dispensed from 3-cc barrels. In dispensing zinc oxide for optical characterization and CHEMFET, 27- and 32-gauge dispensing tips were used, respectively. Substrates were placed on a temperature controlled vacuum chuck which allows control of the substrate deposition temperature from -60 to $+130^\circ\text{C}$. Immediately after the dispensing operation, substrates with zinc oxide precursor features were annealed at 400°C in air for 5 min. CHEMFET with these ZnO film structures were then annealed in a 3% hydrogen–nitrogen gas mixture for 15 min at 400°C.

Profiles of the deposited zinc oxide dots were measured using a Dektak 8000 profilometer (Sloan Technology, Santa Barbara, CA). A sub-micron diamond stylus was used with 0.01 mN of applied force.

Optical transmission and reflectance measurements were obtained between 200 and 3300 nm using a Varian Cary 5 double beam spectrophotometer. Ellipsometry measurements were taken with a ISA J-Y Uvisel phase modulated spectroscopic ellipsometer. Data was recorded from 0.8 to 3.3 eV with a step size of 0.05 eV. A 70° angle of incidence and an integration time of 1 s per point were used. A piece of flat black tape was posted on the back of the transparent silica samples to frustrate the back reflection of the probe beam. Data was analyzed with UVISEL Ellipsometric Software, Version 4.15 [17].

2.3. Sensor microfabrication and testing

The dual-gate CHEMFET with $\text{SiO}_2/\text{Si}_3\text{N}_4$ gate insulator were fabricated at the University of Utah as described previously [18]. On both sides of each CHEMFET channel area, two parallel Pt metallization lines approximately 165 μm apart were formed. Zinc oxide was deposited onto the Si_3N_4 surface over the channel area and Pt metallization lines, thereby forming the transistor gates. This configuration facilitates work function and resistance change measurements on the same ZnO gate. The CHEMFET with deposited ZnO films were attached with conducting epoxy to 16-pin TO-8 headers, ultrasonically wirebonded with Au wires, and tested.

TO-8 headers with mounted CHEMFET chips were placed in a temperature controlled stainless steel flow cell. An automated gas mixing system [19] was used to generate dilutions of hydrogen and ammonia in synthetic hydrocarbon free grade air. 2.74% H_2 and 3.09% NH_3 were purchased from Norco (Boise, ID). CHEMFET sensors with doped zinc oxide films were operated in the drain current mode. Preset drain current was maintained by regulating the gate voltage. The data acquisition sampling rate was programmed to 5 s. The measurements consisted of an initial exposure to carrier gas (synthetic air) for 5 min followed by 10-min exposures to H_2 or NH_3 .

3. Results and discussion

A photograph and a cross section of an Au-doped ZnO film deposited on an oxidized silicon substrate using the automated fluid dispensing method are shown in Fig. 1a and b. In the automated fluid dispensing technique, the layer thickness and uniformity depend on the properties of the fluid and substrate as well as the dispensing parameters used [20]. Fluid viscosity has a major effect. When zinc oxide is dispensed from precursors containing aqueous solutions of ethanol, the strong dependence of the viscosity and surface tension

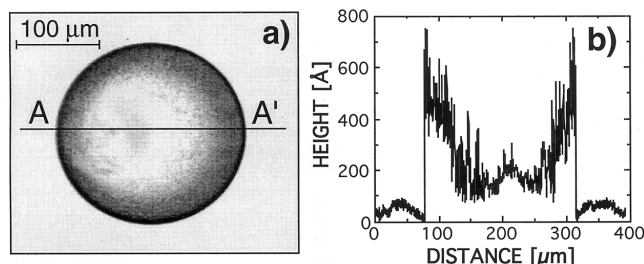


Fig. 1. (a) Photograph of an Au-doped ZnO dot deposited on a silicon wafer at a substrate deposition temperature of 6°C. (b) Cross-section of the dot (A–A') as determined by profilometry.

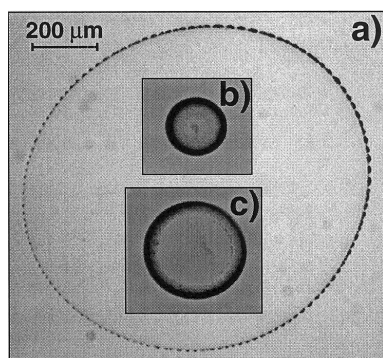


Fig. 2. Photographs of Au-doped ZnO dots deposited on a silicon wafer at 24°C from ZnO solution diluted 1:10 with (a) ethanol; (b) 50% ethanol and water; (c) water.

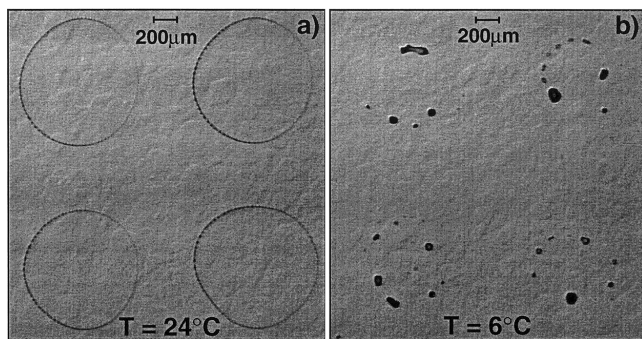


Fig. 3. Photographs of Au-doped ZnO dots deposited on a silicon wafer from the ZnO solution diluted 1:10 with ethanol at the substrate deposition temperature of (a) 24°C; (b) 6°C.

on the ethanol–water ratio can be exploited. At 25°C, the viscosities of ethanol and water are 1.07 and 0.89 mN s m^{−2}, respectively. However, at the same temperature, the viscosity of 50% ethanol and water solution is 2.36 mN s m^{−2} [21]. The surface tensions of ethanol and water are 22.75 and 72.75 mN m^{−1} at 20°C, respectively, while the 48% ethanol solution has a tabulated value of 30.10 mN m^{−1} [22]. The effect of these variations in surface tension and viscosity on dispensing ZnO films is demonstrated in Fig. 2. The original Au-doped ZnO solution was diluted 1:10 with ethanol (Fig. 2a), with 50% ethanol and water (Fig. 2b), or with water (Fig. 2c). Dilution with ethanol results in dots approximately 150 Å thick (measured in the center of the dot) and 1000 μm in diameter while dilution with 50% ethanol and water yields dots approximately 250 Å thick and 180 μm in diameter. Intermediate dots approximately 200 Å thick and 300 μm in diameter are formed from a solution diluted with water.

Large effects of the substrate deposition temperature on the dispensed dot can be observed. An example is discussed for the films deposited from the ethanol–diluted ZnO solution. At a substrate deposition temperature of 24°C, the dots remained characteristically large and thin throughout the deposition, and no fragmentation was observed (Fig. 3a). At a substrate deposition temperature of 6°C, the dispensed dots spread to a thin film, then quickly broke apart into smaller dots arranged along the perimeter of the original dot (Fig. 3b). This behavior can be explained by the temperature dependence of the viscosity, surface tension, and solvent evaporation rate. When the ZnO solution kept at r.t. is dispensed onto a substrate maintained of 6°C, the surface tension and viscosity of ethanol increase as dot temperature decreases. In addition, a slower evaporation rate leaves a larger window for dewetting, and the dot fragments.

For optical characterization by transmission, reflection, and ellipsometry, large diameter zinc oxide dots were required. Therefore, ethanol diluted solutions and a 24°C substrate deposition temperature were used. Using automated fluid dispensing, multiple layers of zinc oxide were deposited on silica and silicon for characterization. The films demonstrated excellent transmission in the visible region, in excess of 85% (Fig. 4). Residual water in the silica substrates resulted in absorption at 1400 and 2200 nm. The characteristic band gap at 380 nm was observed by a decrease in transmission below 5%. Reflectance measurements of films on silicon paralleled these results.

Ellipsometry data and subsequent modeling (Fig. 5) on single and multilayer films yield a refractive index of 2.01 and an absorption coefficient of 0.011 at 500 nm. Modeling was performed on raw ellipsometry data acquired from single and multilayer ZnO films on silica. A classical dispersion relationship for a homogeneous

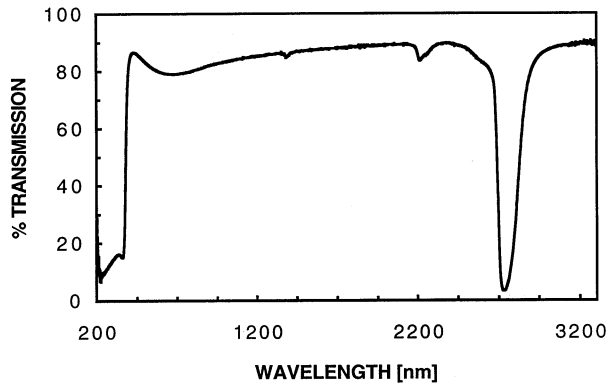


Fig. 4. Optical transmission spectrum of ZnO films deposited on silica. The features near 1400, 2200, and 2750 nm arise from fundamental and overtone vibrations resulting from residual -OH in the silica substrate.

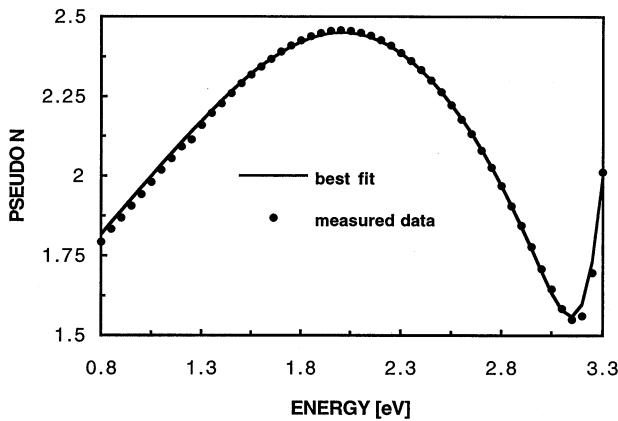


Fig. 5. A selected modeled fit of an ellipsometric trace of the Au-doped ZnO thin film deposited on silica and annealed at 300°C for 1 h in air; $\chi^2 = 0.507$. Fitting parameters: thickness = 840 Å, $\epsilon_\infty = 3.34$, $\epsilon_s = 3.75$, $\omega_o = 3.54$, $\Gamma = 0.135$.

layer resting on a smooth silica substrate was used. A surface roughness was imposed on the ZnO film layer which was parameterized from SEM data. A hemispheric morphology was used with a radius of 10.5 nm and a center to center separation of 21.0 nm. Film thickness was estimated from profilometry measurements. The dispersion relationship is shown in Eq. (1), where $\langle \epsilon \rangle$ is the complex dielectric constant, ϵ_∞ is the high frequency dielectric constant, ϵ_s is the static dielectric constant, ω_o is the oscillator resonance frequency, Γ is the oscillator linewidth, and ω is the frequency.

$$\langle \epsilon \rangle = \epsilon_\infty + (\epsilon_s - \epsilon_\infty) / \{ (\omega_o - \omega) + i\Gamma\omega \} \quad (1)$$

The Bruggeman effective median approximation was used, and the film thickness was allowed to vary as well. The model was used to simulate the measured optical constants as a function of photon energy. The best fit corresponded to a minimum value of χ^2 . Results of the modeling yielded calculated values of the refrac-

tive index (n), the extinction coefficient (k), and the film thickness (Fig. 6). Results were in accord with those reported for spin coated ZnO films [13].

For depositing Au- or Ga-doped ZnO films on CHEMFET sensors with a channel width of 400 μm , dots with diameter around 450 μm were required. Therefore, a water diluted solution was used, and the dot diameter was fine-tuned by the substrate temperature. The conductivity of spin-cast and rf sputtered ZnO films has been found to increase upon reduction in hydrogen [23]. We have followed this procedure with the dispensed ZnO films. As deposited, the resistance of Au- and Ga-doped films measured on CHEMFET was 3.9×10^7 and $5.9 \times 10^5 \Omega$, respectively. After annealing in hydrogen, the resistance of the films decreased to 3.1×10^7 and $1.1 \times 10^5 \Omega$, respectively. After reducing, the CHEMFET with ZnO films were wire-bonded and exposed to hydrogen and ammonia at 120°C. Fig. 7 shows WF responses of the Au-doped ZnO film to ammonia in air over the concentration range from 100 to 10000 ppm. As anticipated, the responses are relatively slow due to the low temperature of the films. Resistance and WF changes of the Au- and Ga-doped ZnO films upon exposure to 1000 ppm of hydrogen and ammonia at 120°C are summarized in Table 1. The Au-doped film gives the same resistance change when exposed either to hydrogen or ammonia while the Ga-doped film gives a larger response upon exposure to

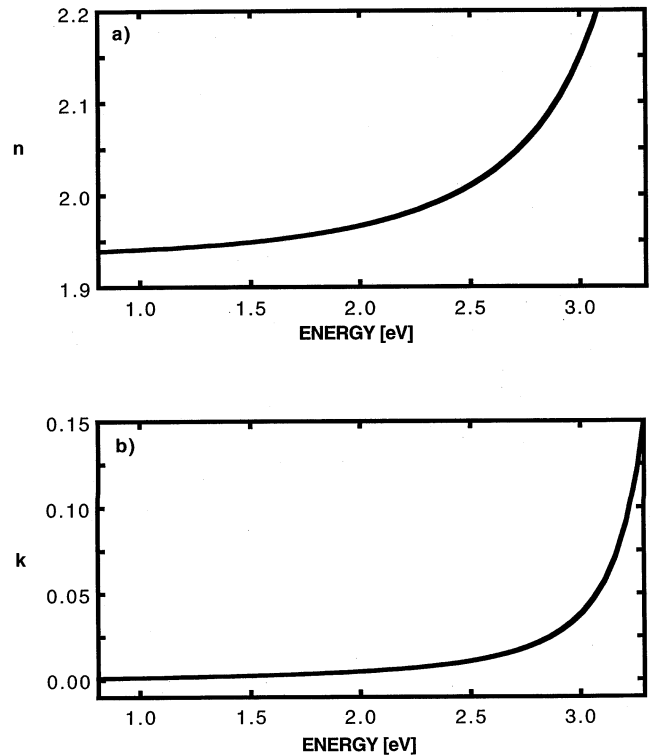


Fig. 6. Plots of refractive index and absorption coefficient versus photon energy as modeled from ellipsometry data.

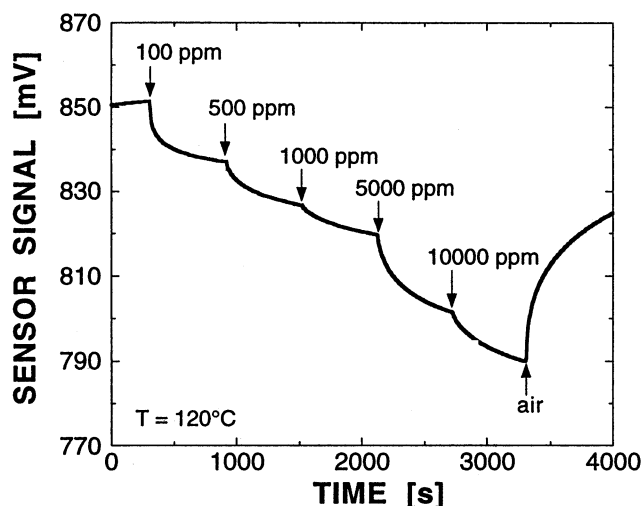


Fig. 7. Work function responses of a CHEMFET with Au-doped ZnO film to ammonia in air.

Table 1

Resistance and work function changes of the Au- and Ga-doped ZnO films upon exposure to 1000 ppm of hydrogen and ammonia at 120°C

Layer	H ₂ (1000 ppm)		NH ₃ (1000 ppm)	
	(R ₀ - R)	ΔWF (mV)	(R ₀ - R)	ΔWF (mV)
	/R ₀ 100 (%)		/R ₀ 100 (%)	
Au-doped ZnO (1 at.%)	14	-10	14	-28
Ga-doped ZnO (1 at.%)	16	-17	6	-27

hydrogen in contrast to ammonia. Work function change in response to ammonia is much more pronounced than to hydrogen.

When interpreting the results in this table, several things must be considered. As mentioned in Section 1, maximum long-term operating temperature of CHEMFET is well below that commonly employed in zinc oxide sensors. As a result, not all responses had reached a steady state value within the 10-min gas exposure time. Also, based on profilometry measurements, Ga doped ZnO layers were more than three times thicker than the Au doped layers, and the Ga doped films exhibited larger surface roughness. These factors influence sensor response and preclude comparing the effects of the different dopants.

Exposure to reducing gases decreases the resistance of the film. These results are consistent with a generally accepted model in which modulation of surface conductivity of zinc oxide by the adsorption of gases and vapors in air is explained through the interaction with surface states associated with adsorbed oxygen [24,25].

Exposure of the zinc oxide surface to reducing species decreases the width of the depletion region. This lowers both work function and resistance. The magnitude of responses depends on the complex interaction of a particular analyte with the surface states and the number of electrons produced from this reaction, among many other factors. Therefore, responses to different reducing gases are expected to vary significantly.

In conclusion, a technique for locally depositing optically clear Au- and Ga-doped zinc oxide films from solution precursors has been demonstrated. Solution-dispersed films have been characterized by means of optical transmission, reflectance, ellipsometry, and profilometry measurements. Employing this method, ZnO films have been deposited on CHEMFET sensors. WF and resistance changes upon exposure to hydrogen and ammonia were measured. Using similar precursors, other target metal oxide films can be deposited by this approach.

Acknowledgements

This work was supported by the US Department of Energy Office of Nonproliferation and National Security, NN-20, and by the Materials Sciences Division of the Office of Basic Energy Science, US Department of Energy. Pacific Northwest National Laboratory is a multiprogram national laboratory operated for the US Department of Energy by the Battelle Memorial Institute.

References

- [1] S. Major, A. Banerjee, K.L. Chopra, *Thin Solid Films* 108 (1983) 333.
- [2] S. Major, A. Banerjee, K.L. Chopra, *Thin Solid Films* 125 (1985) 179.
- [3] P. Pushparajah, A.K. Arof, S. Radhakrishna, *J. Phys. D Appl. Phys.* 27 (1994) 1518.
- [4] T. Minami, H. Sato, H. Sonohara, S. Takata, T. Miyata, I. Fukuda, *Thin Solid Films* 253 (1994) 14.
- [5] H. Nanto, T. Minami, S. Shooji, S. Takata, *J. Appl. Phys.* 55 (1984) 1029.
- [6] S. Takada, *J. Appl. Phys.* 73 (1993) 4739.
- [7] P. Petrou, S. Singh, D.E. Brodie, *Appl. Phys. Lett.* 35 (1979) 930.
- [8] V. Craciun, J. Elders, J.G.E. Gardeniers, I.W. Boyd, *Appl. Phys. Lett.* 65 (1994) 2963.
- [9] G.J. Exarhos, S.K. Sharma, *Thin Solid Films* 270 (1995) 27.
- [10] D.L. Polla, R.S. Muller, R.M. White, *IEEE Electron Device Lett.* EDL-7 (1986) 254.
- [11] J. Suehle, R.E. Cavicchi, M. Gaitan, S. Semancik, *IEEE Electron Device Lett.* 14 (1993) 118.
- [12] G.J. Exarhos, L.Q. Wang, T. Dennis, *Thin Solid Films* 253 (1994) 41.
- [13] A. Rose, G.J. Exarhos, *Thin Solid Films* 308 (1997) 42.
- [14] J. Janata, in: J. Janata, R.J. Huber (Eds.), *Solid State Chemical Sensors*, Academic, New York, 1985, p. 65.

- [15] H. Nanto, T. Minami, S. Takata, J. Appl. Phys. 60 (1986) 482.
- [16] S. Pizzini, N. Butta, D. Narducci, M. Palladino, J. Electrochem. Soc. 136 (1989) 1945.
- [17] UVISEL, Ellipsometric Software, Version 4.15, Instruments, S.A./Jobin-Yvon, Edison, NJ, 1996.
- [18] R.J. Huber, in: J. Janata, R.J. Huber (Eds.), Solid State Chemical Sensors, Academic, New York, 1985, p. 119.
- [19] K. Domansky, D.L. Baldwin, J.W. Grate, T.B. Hall, J. Li, M. Josowicz, J. Janata, Anal. Chem 70 (1998) 473.
- [20] K. Domansky, E.A. Watters, Proceedings of the Symposium on Microstructures and Microfabricated Systems, Montreal Quebec, Canada, vol. 97-5, Electrochemical Society, Pennington, NJ, 1997, p. 144.
- [21] D.R. Lide (Ed.), CRC Handbook of Chemistry and Physics, CRC Press, Boca Raton, FL, 1993, p. 6–198.
- [22] R.C. Weast (Ed.), Handbook of Chemistry and Physics, CRC, Boca Raton, FL, 1980, p. F-45.
- [23] G.J. Exarhos, A. Rose, C.F. Windisch, Thin Solid Films 308 (1997) 56.
- [24] G. Heiland, Sens. Actuators 2 (1982) 343.
- [25] S.R. Morrison, Sens. Actuators 2 (1982) 329.